Establishment and characterization of patient-derived primary cell lines as preclinical models for gallbladder carcinoma

Feiling Feng[1#], Chuncui Huang[2#], Mingjia Xiao[1#], Huizhen Wang[3#], Qingxiang Gao[1], Zishuo Chen[3], Xiaoya Xu[3], Jun Zhou[3], Fugen Li[3], Yan Li[4], Dadong Zhang[3], Yanxin Chang[5], Xiaoqing Jiang[1]

[1]Department of Biliary I, Shanghai Eastern Hepatobiliary Surgery Hospital, Navy Military Medical University, Shanghai 200438, China; [2]Institute of Biophysics, Chinese Academy of Sciences, Beijing 100101, China; [3]Research and Development Institute of Precision Medicine, 3D Medicines Inc., Shanghai 201114, China; [4]University of Chinese Academy of Sciences, Beijing 100049, China; [5]Biliary Tract Surgery Department, Shanghai Eastern Hepatobiliary Surgery Hospital, Navy Military Medical University, Shanghai 200438, China

Contributions: (I) Conception and design: D Zhang, Y Chang, X Jiang; (II) Administrative support: F Li, Y Li; (III) Provision of study materials or patients: F Feng, M Xiao, Q Gao; (IV) Collection and assembly of data: Z Chen, X Xu, J Zhou; (V) Data analysis and interpretation: F Feng, C Huang, M Xiao, H Wang; (VI) Manuscript writing: All authors; (VII) Final approval of manuscript: All authors.

#These authors contributed equally to this work.

Correspondence to: Professor Xiaoqing Jiang, MD. Department of Biliary I, Shanghai Eastern Hepatobiliary Surgery Hospital, Navy Military Medical University, 225 Changhai Road, Shanghai 200438, China. Email: xqjiang_dandaoyike@163.com; Yanxin Chang, MD. Biliary Tract Surgery Department, Shanghai Eastern Hepatobiliary Surgery Hospital, Navy Military Medical University, Shanghai 200438, China. Email: pycmu402@163.com; Dadong Zhang, PhD. Research and Development Institute of Precision Medicine, 3D Medicines Inc., Room 201, Building 2A, No. 158 Xin Junhuan Road, Pujiang Hi-tech Park, Shanghai 201114, China. Email: dadong.zhang@3dmedcare.com.

Background: Gallbladder carcinoma (GBC) is one of the most lethal malignancies which do not have a targeted drug in the clinic. Patient-derived primary cell lines (PDCs) are useful in assessment of cancer complexity and heterogeneity, drug-sensitivity tests, and personalized-drug-selection guidance. The aim of this study is to establish GBC PDCs and characterize their biological features.

Methods: The characterization of PDCs was defined by morphology, growth kinetics, chromosomal analysis, short tandem repeat (STR) analysis, RNA-seq and tumorigenicity. Glycosylation of PDCs derived from GBC was first studied, and the PDC model's performance were also tested and evaluated using seven molecular target inhibitors.

Results: Three novel GBC cell lines from three GBC patients were successfully established and denoted as JXQ-3D-902R4, JXQ-3D-4494R, and JXQ-3D-4786R. These cell lines demonstrated the heterogeneous characteristics of tumor morphology and phenotypes which are consistent with primary GBC, such as irregular cell shape, varied chromosomal numbers, and different STR patterns. Moreover, the growth activity and tumorigenicity ability varied among the cell lines, of which JXQ-3D-4494R exhibited the best growth rate. Furthermore, glycan profiling of whole proteins were detected and characterized. Unique N-glycans of each PDC were identified, JXQ-3D-902R4, JXQ-3D-4494R and JXQ-3D-4786R contained ten, four and seven unique glycans, respectively. The epithelial origins of three PDCs were confirmed using RNA-seq based on the highly expressed typical epithelial marker genes. Moreover, the drug-sensitivity results demonstrated that the three PDCs exhibited different responses to the seven-most commonly used targeted medicines belonging to three groups: cell-cycle inhibitors, PI3K/AKT/mTOR signaling-pathway inhibitors, and ErbB inhibitors. JXQ-3D-4494R was sensitive to most of the inhibitors, JXQ-3D-4786R was sensitive to ErbB inhibitors, and JXQ-3D-902R4 was sensitive to PI3K/AKT/mTOR inhibitors.

Conclusions: These results indicate that PDCs may be efficient preclinical models for further investigation of the biological behaviors and potential targeted therapies of human GBC.

Keywords: Gallbladder carcinoma (GBC); patient-derived primary cell line (PDC); glycosylation; preclinical model; drug sensitivity

Introduction

Gallbladder carcinoma (GBC), the most common primary biliary tract cancer (BTC), is one of the most lethal malignancies, which is generated from the gallbladder or cystic duct. GBC accounts for nearly two-thirds of BTCs and is the sixth-most common gastrointestinal tract cancer (1), and is characterized by its aggressive growth and high lethality. In China, GBC is the fifth-ranked cancer of the gastrointestinal tract. The age of high incidence is 50–75 years old, and its incidence in females is about two-fold higher than that of males (2,3). The onset of GBC is insidious, difficult to diagnose early, exhibits a high degree of malignancy, and is prone to early metastasis. Consequently, GBC generally carries an extremely poor prognosis because the majority of patients are at an advanced stage at the initial diagnosis. The 5-year survival rate of GBC is between 5% and 10% at advanced stages (4).

Currently, surgical resection in combination with neoadjuvant or adjuvant therapies is still the only potentially curative modality for resectable GBC patients to achieve long-term survival (5). However, GBC resection rate was 69.7%, and the rate of curative resection was 37.7% from 1998 to 2004 in Japan (6). Unfortunately, only a small proportion of GBC patients are eligible to receive surgical intervention due to organ or liver invasion starting from a relatively early stage (7). A standard treatment for GBC has not yet been established (8,9). Although advances in many therapeutic strategies against GBC have been developed, the prognosis for the majority of patients with GBC has not improved appreciably (9). Therefore, it is important to investigate the specific biological mechanisms underlying GBC and to evaluate the sensitivity of potential drugs to treat GBC.

Recently, patient-derived primary cell lines (PDCs) have been developed and characterized as tumor models for cancer research (10). PDCs, which are isolated directly from resected tumor tissues, have a finite lifespan and limited expansion capacity, maintaining many of the important markers and functions seen in original tissues (11,12). PDC models retain the principal histologic and genetic characteristics of donor tumors and remain stable throughout passages, and are also used to predict clinical outcomes used for preclinical drug evaluation, biomarker identification, biological studies, and personalized-medicine strategies (13-15). Thus, PDC models are useful for assessment of the complexity and heterogeneity of GBCs, test-drug sensitivities, and for guiding personalized-drug selection for each patient. At present, there are few established GBC cell lines derived from primary tumors (16), and no studies have characterized glycosylation in these GBC cell lines.

Glycosylation is one of the most common post-translational protein modifications and is associated with several pathophysiological processes. Aberrant glycosylation may lead to the development of cancer. It have been reported that fucosylation of prostate-specific antigen (PSA) can be used to differentiate aggressive and non-aggressive prostate cancer (17). Moreover, changes in glycan patterns may contribute to identifying stages of colorectal cancer (CRC). The carcinoembryonic-antigen (CEA) glycan levels of N-acetylgalactosamine, mannose, and galactose during stage-II CRC have a significant downward trend compared with those at other stages. Thus, these altered glycans may be indicative of the progression of tumor development (18). Furthermore, N-glycan profiling may help in the determination of the origin of a carcinoma and may help to differentiate normal cells from cancer cells. It has been reported that high-mannose-type and core-fucosylated N-glycans are higher in bladder cells than in normal cells (19). The study of various CRC cell lines has also demonstrated that bisecting N-acetylglucosamine is expressed at a high level in the CRC cell line, LIM1215 (20). Thus, these glycans may serve as molecular markers to differentiate different stages of cancer.

Our previous study has demonstrated that three PDCs, derived from the same patient with gallbladder sarcomatoid carcinoma, could be applied to elucidate the sensitivity of cells to targeted agents (21). In this study, we further established three PDCs using fresh primary tumor cells from three surgically resected patients with GBC. Here, we characterized three new human GBC cell lines, including their glycosylation features, and also examined their responses to the seven-most commonly used targeted therapeutic agents. The three novel PDCs could be an

ideal tool for further investigation of the tumor biology and potential treatment of GBC.

Methods

PDC establishment and cell culture

The entire process of PDC establishment was sterile. Fresh gallbladder adenocarcinoma tissues from three patients were washed by cold sterile phosphate buffered saline (PBS) to remove excess blood and connective tissue. Then the tissues were cut into 1 mm³ pieces and washed by cold sterile PBS several times. All pieces were placed in 10 cm² dishes and incubated in DMEM/F12 complete growth medium which consisted of 90% DMEM/F12 (Gibco™, C11330500BT) with 10% fetal bovine serum (FBS) (Gibco; Thermo Fisher Scientific, Inc., Waltham, MA, USA), and with 1% non-essential amino acids (Gibco™, 11140076) and 1% penicillin (100 U/mL)/streptomycin (100 µg/mL) (Gibco™, 15140-122; Thermo Fisher Scientific, Inc.). When the cells reached approximately 30% confluency, the supernatant and excessive tissues were removed and the cells were detached by 0.25% trypsin-EDTA (Gibco™, 25200072; Thermo Fisher Scientific, Inc.) and transferred into 24-well plates. After 5–6 passages tumor cells were effectively purified, then the cells were scale-up cultured in DMEM/F12 complete growth medium and were grown in a 37 7 incubator with 5% CO_2. After establishment, the three PDCs were stored at low passages. The passage of each PDC used in the following experiment was different and the passage information for each PDC in the assays ranged between 15 and 30.

Cell morphology, karyotypes and short tandem repeat (STR) analysis

The morphologies of three PDCs (JXQ-3D-4494R, JXQ-3D-4786R and JXQ-3D-902R4) were detected by microscopy. Pictures at 40×, 100× and 200× magnifications were taken after changing media after every passage at an appropriate cell density. Subsequently, karyotype analysis and STR sequence were detected before experiments to ensure that the cells were homogeneous. Three PDCs (JXQ-3D-4494R, JXQ-3D-4786R and JXQ-3D-902R4) were trypsinized and plated to new 10 cm² dishes. The medium were changed with the addition of 0.2 µg/mL colchicine when the cells reached 80–90% confluence. After 1 h

incubation at 37 ℃, the cells were trypsinized, centrifuged and resuspended gently with 7 ml pre-warmed 0.075 mol/L KCl solution and incubated for 20 minutes in a 37 ℃ water bath. After 3 minutes pre-fixed by addition of 1 mL Carnoy's Fluid, the cells were centrifuged at 1,200 rpm for 5 minutes, resuspended gently with 7 mL fresh Carnoy's Fluid and incubated for 40 minutes in a 37 ℃ water bath. Then the cells were centrifuged and resuspended with about 500 µL Carnoy's Fluid to an appropriate cell concentrate. Then the suspension were dropped to pre-cooled slices and dried quickly. The slices were stained with 10% Giemsa for 10 minutes. Pictures of 40× were taken for at least 20 metaphase cells with a microscope after the slices were dried. Three PDCs (JXQ-3D-4494R, JXQ-3D-4786R and JXQ-3D-902R4) and their origin tissues were taken STR profiling analysis for 20 loci by Shanghai Biowing Applied Biotechnology Co. Ltd.

Colony-formation assay

Cells were plated at 500 cells per well in six-well plates with complete DMEM/F12 medium and were incubated in a 37 ℃ incubator with 5% CO_2 for 10 days. On day 10, the cells were rinsed with PBS and fixed with methanol for 10 min. Then, the cells were stained with 0.1% crystal violet for 10 min and the numbers of colonies were counted.

Cell proliferation assay

Three PDCs (JXQ-3D-4494R, JXQ-3D-4786R and JXQ-3D-902R4) and no-cell controls were plated in six 96-well plates and were biologically replicated across three wells. Three PDCs were cultured in three densities at 4,000, 2,000 and 1,000 cells/well to determine the optimal plating density. The experimental design is shown in *Figure S1*. For plates that required incubation times that were longer than 48 h, the medium was replaced every 48 h. The entire incubation process was maintained under sterile conditions during addition of reagents and incubations to avoid microbial contaminants. The number of viable cells from each plate was determined at 24, 48, 72, 96, 120 and 144 h by alarma blue (kept from direct light) and the fluorescence was determined at 530–560 nm excitation wavelength and 590 nm emission wavelength by a microplate reader after a 90 min incubation at 37 ℃. Then, Graphpad Prism5 software was used to calculate the population-doubling times of each cell line at different cell densities. With

the assumptions that all cells grew exponentially and that growth consisted of a constant doubling time, nonlinear regression was chosen to analyze population-doubling times.

RNA-sequencing

RNA-seq was performed as previously described (22). Randomly interrupted mRNA and the first strand cDNA were synthesized, and then a second cDNA strand was synthesized. RNA-seq library construction, hybrid capture and sequencing were performed at WuXi Next CODE (Shanghai, China). RNA-seq was performed using an Illumina HiSeq X Ten PE150 instrument.

N-glycosylation modification of proteins assay

Whole proteins from cells were extracted with density-gradient centrifugation and differential centrifugation technology. After harvesting and washing 1×10^7 cells in PBS, the cell pellets were resuspended in a homogenization buffer consisting of 0.25 M sucrose, 20 mM HEPES-KOH, and pH 7.4 with a protein-inhibitor cocktail before freezing and thawing the samples. Cell lysates were centrifuged at 2,000 g for 10 min to remove insoluble cell debris before ultra-centrifugation at 200,000 g for 45 min at 4 ℃ to collect the cytosolic fractions. Second step, release N-glycans. Glycoproteins were first reduced and carboxymethylated in the presence of dithiothreitol (DTT) and iodoacetamide (IAA) followed by dialysis in 50 mM Ambic buffer for 24–48 h at 4 ℃. Glycoproteins were then digested by trypsin at 37 ℃ overnight. The resulting glycopeptides were applied to a Sep-Pak C18 cartridge which was conditioned successively with 5% acetic acid and 100% propan-1-ol, and eluted stepwise with 20% and 40% propan-1-ol solution. The propan-1-ol fractions were digested with PNGase F (New England BioLabs, Inc., Ipswich, MA, USA) at 37 ℃ for 20–24 h. Separation of the *N*-glycans from the digestion mixture was made by using the C18 Sep-Pak and the solvent system propan-1-ol/5% acetic acid. Last, multistage matrix-assisted laser desorption/ionization time of flight mass spectrometry (MALDI-TOF-MS) analysis (23). Lyophilized derivatization N-glycans were resuspended in 10 μL methanol. Then a 1 μL aliquot and 20 mg/mL dihydroxybenzoic acid (DHB) were spotted on a stainless-steel μFocus MALDI target plate and mixed well. After being air-dried, the obtained N-glycans were characterized by MALDI-TOF-MS.

Tumorigenesis ability of PDCs

Three PDCs (JXQ-3D-4494R, JXQ-3D-4786R and JXQ-3D-902R4) were trypsinized, counted and diluted into 1×10^7 cells/75 μL with complete culture media. Then, an equal volume of matrix gel was mixed with the cell suspension on ice to generate a suspension with a density of 1×10^7 cells/150 μL. The cell suspension was subcutaneously injected into four sites, including both flanks of the scapula and the outer thigh of 4-weeks-ol female Balb/c nude mice (Shanghai Slake Experimental Animal Co., LTD) for 150 μL per site. Tumor sizes were measured once a week and calculated by volume = width^2 × length/2. The mice were sacrificed when the tumor reached ~1,000 mm^3. All animal experiments and procedures were carried out in accordance with the institutional protocol approved by the Medicine Institutional Animal Care.

In vitro anti-proliferation assay of PDCs

The three PDCs were further characterized by analyzing their responses to chemo-agents. Seven compounds (ribociclib, palbociclib, MK2206, everolimus, PI-103, lapatinib and dacomitinib) were tested. A vehicle control and positive control were also produced at the same time. The seven compounds were first dissolved in DMSO, and then each compound was diluted into nine doses by gradient dilution at a gradient of 1:3.16. Then, the compounds were sequentially diluted by DMEM/F12 complete growth medium to the final concentration 10×. The maximum concentration of the nine doses for the seven compounds was as follows: ribociclib (100 μM), palbociclib (200 μM), MK2206 (30 μM), everolimus (1 μM), PI-103 (50 μM), lapatinib (50 μM) and dacomitinib (100 μM). The original cell density of three PDCs were as follows: JXQ-3D-4494R, 1,000 cells/well; JXQ-3D-4786R, 4000 cells/well; and JXQ-3D-902R4, 2,000 cells/well. Cell viability was measured using a Cell Titer-Glo Luminescent Cell Viability Assay (Promega, USA) after 144 h incubation. Additionally, the 50% inhibition of cell viability (IC50) was calculated from a four-parameter curve analysis and was determined from a
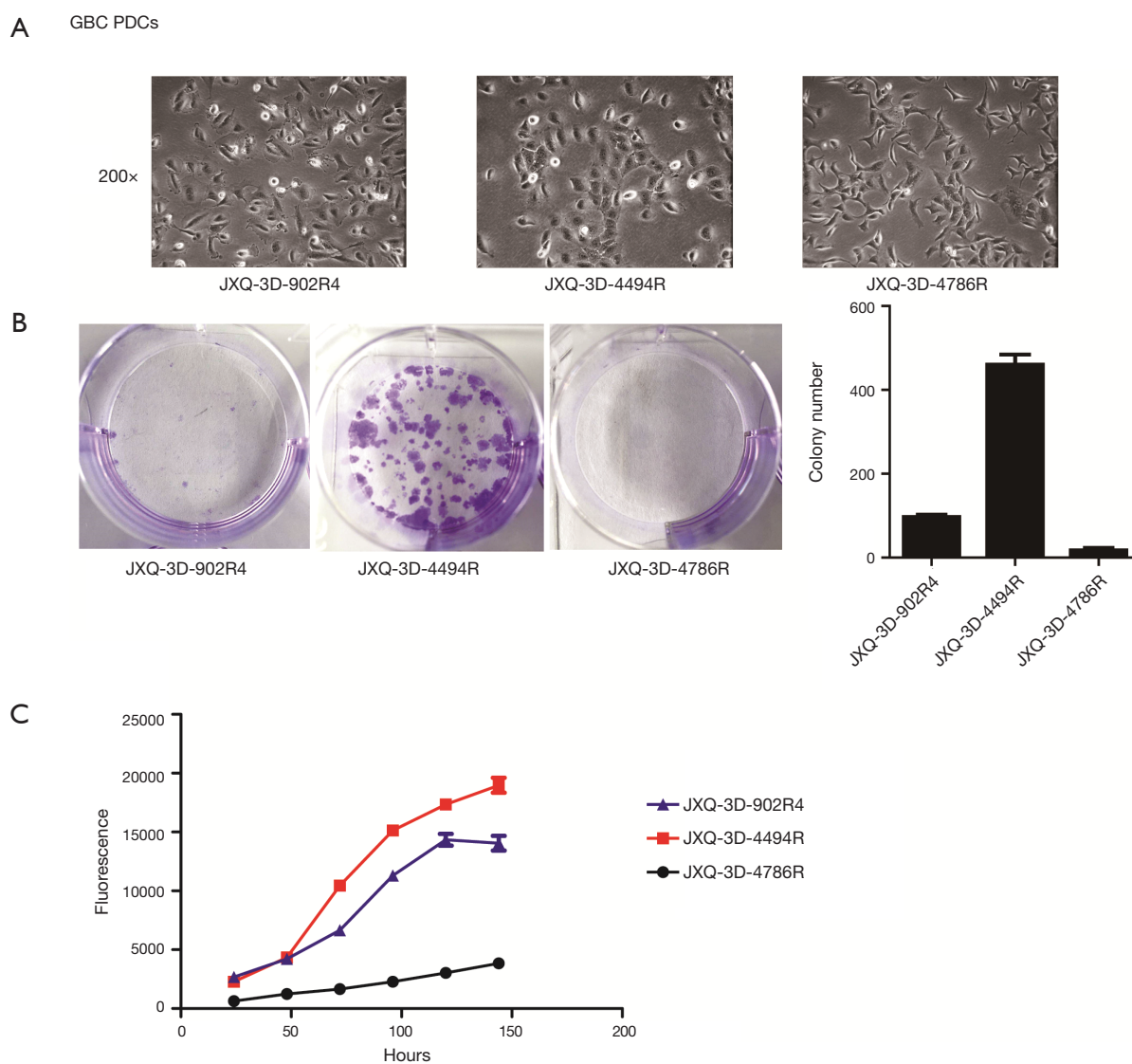
Figure 1 Biological characteristics of three GBC PDCs. The three GBC PDCs (JXQ-3D-902R4, JXQ-3D-4494R, and JXQ-3D-4786R) were derived from three gallbladder adenocarcinoma patients. The cell morphology (A), colony formation activity (B), and proliferation (C) of three GBC PDCs are shown. For colony formation assay (B), a colony is defined as a cluster of approximately 50 cells which can often be determined microscopically. For cell proliferation assay (C), the fluorescence of y-axis represented the cell densities of three PDCs at origin cell density of 2,000 cells/well. Magnification, 200×. Error bars represent mean +/– SD from three replicates. GBC, gallbladder carcinoma; PDC, patient-derived primary cell line; SD, standard deviation.

minimum of three experiments.

Results

Establishment of GBC PDCs

Three PDCs were successfully established *in vitro* from human tumor tissues which were obtained from surgically resected specimens of three GBC patients, who were further diagnosed as gallbladder adenocarcinoma by pathologists. The three novel GBC PDCs were denoted as JXQ-3D-902R4, JXQ-3D-4786R and JXQ-3D-4494R, which were derived from different sites of the three GBC patients (*Figure 1A*). The patients did not receive any intervention or treatment before surgery. The clinical characteristics of

Table 1 Clinical information of three patients with gallbladder adenocarcinoma*

Cell line	Clinical pathological diagnosis	Sex	Age	Site	Size	TNM	Tumor staging	CEA (ng/mL)	CA19-9 (U/mL)	CA125 (U/mL)	CA72-4 (U/mL)	AFP (ng/mL)	Total bilirubin (µmol/L)	TBA (µmol/L)
JXQ-3D-902R4	Gallbladder adenocarcinoma	Female	60	Gallbladder	10 cm	T3N0M0	IIIa	1.5	34.4	113.8	1.5	2.2	11.4	3.2
JXQ-3D-4494R	Gallbladder adenocarcinoma	Male	65	Gallbladder	5 cm	T3N0M1	IVb	1.5	7.7	18.8	2.3	2.2	6.4	5.6
JXQ-3D-4786R	Gallbladder adenocarcinoma	Male	69	Gallbladder	1.9 cm	T3N0M0	IIIa	10.9	143.9	22.4	1.5	2.9	215.4	114.2

*All three patients were initially diagnosed with gallbladder adenocarcinoma, and they did not receive any intervention or treatment before surgery. TNM, tumor, nodes, metastasis; CEA, carcinoembryonic antigen; CA, carbohydrate antigen; AFP, alpha fetoprotein; TBA, total bile acid.

Table 2 Karyotype analysis of three newly established PDCs

Cell line	Karyotype information* (number of chromosomes/number of cells)
JXQ-3D-902R4	70/1, 71/4, 72/2, 73/1, 74/1,75/2, 76/2, 78/1, 80/4, 81/1, 83/1
JXQ-3D-4786R	54/1, 56/1, 57/1,58/2, 59/1,60/2,61/1, 62/3, 63/2, 64/2, 65/1, 66/1, 67/1, 68/1
JXQ-3D-902R4	43/1, 44/1, 46/1, 47/2, 48/3, 49/4, 50/3, 51/4, 52/1

*Karyotype analysis of three newly established PDCs was carried out in metaphase in cell division, and 20 cells for each PDC were lysed and the chromosomes were counted. The chromosomes' distribution according the numbers is shown in the table. PDCs, patient-derived primary cell lines.

the GBC patients related to the three PDCs are listed in *Table 1*.

Characterization of GBC PDCs

The morphological characteristics of the three PDCs were observed under phase-contrast microscopy *in vitro*. All three cultured tumor cells grew in monolayer sheets and adhered strongly to the bottom of dishes. The morphology of three PDCs was a little different. JXQ-3D-902R4 grew in irregular-shaped, partially-fusiform, spindle-shaped single cells varying slightly in size. JXQ-3D-4786R grew mainly in clusters of long polygonal cells that formed branches in many directions, and the morphology of JXQ-3D-4494R was quite different since it exhibited short blunt round-shaped single cells, which were clustered in a way that mimicked pavement confluency in appearance (*Figure 1A*).

Chromosomal aberrations were observed in all three PDCs. Chromosomal analyses revealed a range of numerical abnormalities with aneuploidy. Most cells of the three PDCs had more than 46 chromosomes except some cells of JXQ-3D-4786R, which had less than 46 chromosomes

(*Table 2*). Variations in chromosomal number are shown in *Table 2*. The chromosomal number of JXQ-3D-902R4 ranged between 70 and 83, with a median of 75, while the chromosomal number of JXQ-3D-4494R was distributed in the range of 54–68 without an obvious mode, but was mainly distributed between 58 and 64. Finally, JXQ-3D-4786R had a modal chromosomal number of 49 to 51 with a range of 43–52 (*Table 2*).

A STR profiling assay of 20 standard STR markers, and Amelogenin gender-determining markers, was performed for the three PDCs (*Table 3*) and their origin tissues (*Table S1*). The marker for Amelogenin demonstrated that the JXQ-3D-902R4 cell line was from female origin with XX chromosomes, whereas JXQ-3D-4494R and JXQ-3D-4786R were of male origin with XY chromosomes. The identification of new cell lines and the assessment of cross-contamination were carried out through the DSMZ database (https://www.dsmz.de/services/services-human-and-animal-cell-lines/online-str-analysis.html). No cross contamination was found for any cell line. The STR results suggest that the three PDCs are novel GBC cell lines. Comparing the STR results of PDCs and the origin tissues

Table 3 DNA fingerprinting analysis using 20 STR loci for three established GBC PDCs

STR locus	JXQ-3D-902R4	JXQ-3D-4494R	JXQ-3D-4786R
Amelogenin	X	X, Y	X, Y
D5S818	11, 12	11, 12	11, 13
D13S317	9, 11	8, 12	8, 10
D7S820	8, 12	8,11	11
D16S539	10, 11	9, 12	10, 13
vWA	19	16	18
TH01	9	7	7
TPOX	8, 12	9, 12	8
CSF1PO	12	9, 12	11, 12
D12S391	20	18, 19	20
FGA	25	23, 27	22, 24
D2S1338	19, 23	19, 23	19
D21S11	31, 32	31	29, 32.2
D18S51	17, 19	17	14
D8S1179	13	12, 15	14
D3S1358	15	18	16, 17
D6S1043	11	18, 19	10
PENTAE	12	12, 21	12, 17
D19S433	15.2	12, 14	13, 15.2
PENTAD	8, 13	9	11, 12

GBC, gallbladder carcinoma; PDCs, patient-derived primary cell lines; STR, short tandem repeat.

showed the PDCs to have been derived from the primary GBC tissues.

After establishment, the growth characteristics of the three GBC PDCs—composed of the proliferation-related properties including cell proliferation and colony formation activities—were studied *in vitro* (*Figure 1B*,*C*). JXQ-3D-4494R had the highest cloning efficiency among the three PDCs (*Figure 1B*); growth curves also showed the same tendency. At the same seeding density of 2,000 cells/well, JXQ-3D-4494R had the fastest growth rate among the cell lines (*Figure 1C*). The population-doubling time for JXQ-3D-902R4 was 42 h at a density of 2,000 cells/well in 96-well plates, 38 h at a density of 1,000 cells/well for JXQ-3D-4494R, and 57 h for JXQ-3D-4786R at a density of 4,000 cells/well.

RNA-seq was performed to identify the gene expression of three PDCs. Each PDC was assessed three times in parallel. The typical epithelial marker genes specifically *KRT7*, *KRT8*, *KRT18* and *KRT19* were more highly expressed than the negative control genes (*CD34* and *VIM*) (*Table S2*).

Glycosylation characteristics of the three PDCs

N-glycans of JXQ-3D-902R4 were shown in *Figure 2A*. Without separation, 30 specific N-glycans (linked to asparagine) of JXQ-3D-902R4 were detected. Among the 30 N-glycans, five were of the high-mannose type, 10 were those of bi-antennary structures, and 15 were those of tri-antennary and tetra-antennary structures. The proposed N-glycans and the assignment of peaks are shown in *Figure 2A*. Interestingly, about half of these N-linked glycans contained one or two residues of sialic acid attached to terminal galactosyl, and more than half of these glycans comprised up to two residues of fucose which are linked to reducing terminal N-acetylglucosaminide and the non-reducing end of the glycans. 17 N-linked glycans were harvested from JXQ-3D-902R4, which equated to almost 57% of the CEA glycan moieties present core fucosylation (attached to GlcNAc) according to the study. Core fucosylation was transferred from fucose of guanosine diphosphate-fucose (GDP-Fuc) to the innermost GlcNAc with the catalysis of core fucosyltransferase. Similarly, both residues of sialic acid and residues of fucose were found in 15 N-linked glycans of tumor antigen.

N-glycans of JXQ-3D-4494R were shown in *Figure 2B*. Without separation, 28 specific N-glycan of JXQ-3D-4494R were detected. Among the 28 N-glycans, five were of the high-mannose type, 11 were those of bi-antennary structures, 10 were of tri-antennary and tetra-antennary structures, and 2 bisected glycans were also determined. The proposed N-glycans and the assignment of peaks are shown in *Figure 2B*. Only 12 glycans contained one or two residues of sialic acid attached to terminal galactosyl, and more than half of these glycans comprised up to two residues of fucose which are linked to reducing terminal N-acetylglucosaminide and the non-reducing end of the glycans. Almost all the fucosylated glycans harvested from JXQ-3D-4494R presented core fucosylation (attached to GlcNAc) according to the study. Similarly, both residues of sialic acid and residues of fucose were found in 11 N-linked glycans of tumor antigen.

N-glcyans from JXQ-3D-4786R were shown in *Figure 2C*. Without separation, 29 specific N-glycan extracted from
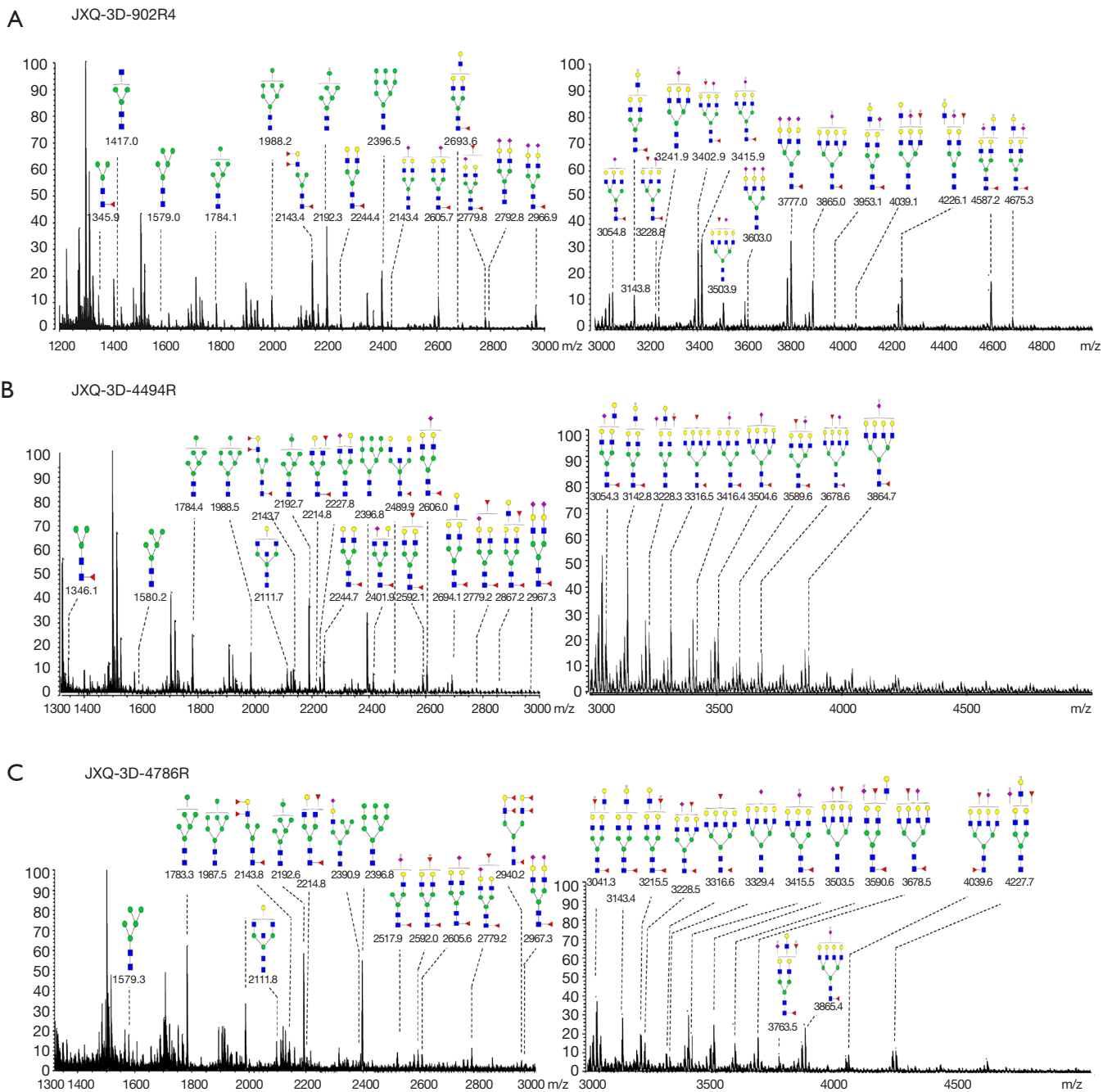
Figure 2 Glycosylation modification of three GBC PDCs. MADLI-TOF-MS was used to analyze the N-glycosylation composition of the whole protein of three GBC PDCs after methylation. N-glycans from GBC patient-derived primary cell line of JXQ-3D-902R4 (A), JXQ-3D-4494R (B), and JXQ-3D-4786R (C), respectively. N-linked glycans were slightly different in amounts for three GBC PDCs, but structures of the glycans were markedly different. Acetylglucosamine (■), Mannose (●), Galactose (●), Fucose (▲), N-acetylneuraminic acid (◆). GBC, gallbladder carcinoma; PDC, patient-derived primary cell line; MADLI-TOF-MS, matrix-assisted laser desorption/ionization time of flight mass spectrometry.

JXQ-3D-4786R were detected. Among the 29 N-glycans, five were of the high-mannose type, 8 were those of bi-antennary structures, and 14 were those of tri-antennary and tetra-antennary structures. One bisected glycan and one hybrid glycan was discovered. The proposed N-glycans and the assignment of peaks are shown in *Figure 2C*. Fifteen glycans contained one or two residues of sialic acid attached to terminal galactosyl, and more than half of these glycans comprised up to two residues of fucose which are linked to reducing terminal N-acetylglucosaminide and the non-reducing end of the glycans. Almost all the fucosylated glycans harvested from JXQ-3D-4786R presented core fucosylation (attached to GlcNAc) according to the study. Similarly, both residues of sialic acid and residues of fucose were found in 13 N-linked glycans of tumor antigen.

Comparisons of N-glycans in different GBC PDCs

N-linked glycans were slightly different in amounts for the three PDCs, but structures of the glycans were markedly different. As shown in *Table 4*, ten unique N-glycans were identified from JXQ-3D-902R4, whereas four were identified for JXQ-3D-4494R, and seven were identified for JXQ-3D-4786R. For the JXQ-3D-902R4 cell line, its unique N-glycans were mostly sialylated. For JXQ-3D-4494R, unique bisecting N-glycans were detected. For JXQ-3D-4786R, unique hybrid and highly fucosylated N-glycans were detected. As a result, these unique features in glycosylation were used to identify cell lines from different patients. In addition, 63% of the glycans were sialyted glycans in JXQ-3D-902R4, whereas there were 42% for JXQ-3D-4494R, and 51% for JXQ-3D-4786R. The ratios of core fucosylated glycans were 56%, 67%, and 62% for JXQ-3D-902R4, JXQ-3D-4494R and JXQ-3D-4786R, respectively.

Tumorigenesis assay in vivo

All three GBC PDCs (JXQ-3D-902R4, JXQ-3D-4494R and JXQ-3D-4786R) were transplanted subcutaneously into nude mice for tumorigenesis observations. Both transplanted xenograft models of JXQ-3D-902R4 and JXQ-3D-4494R showed kinetic growth curves (*Figure 3*). Transplanted xenografts of JXQ-3D-902R4 grew up to over 500 mm^3 on day 44 after injection, while the ones of JXQ-3D-4494R grew up to a similar tumor volume on day 20 after injection (*Figure 3*). Finally, JXQ-3D-4786R did not grow to form any tumors *in vivo*. These results imply

that JXQ-3D-4494R possesses the strongest tumorigenic ability among the three GBC PDCs. The tumorigenesis of the three PDCs also yielded the same trend similar to that of their growth activity results. Images of transplanted xenografts of JXQ-3D-902R4 and JXQ-3D-4494R were also shown (*Figure S2*).

Diverse responses of the three PDCs to targeted drugs

The three established GBC PDCs were used as *in vitro* models to study the sensitivity of targeted medicines. In the present study, seven molecular target inhibitors were used for PDCs model performance testing and evaluation: ribociclib, palbociclib, MK2206, everolimus, PI-103, lapatinib and dacomitinib. Ribociclib and palbociclib were examples of cell cycle inhibitors, whereas MK2206, everolimus and PI-103 were representative as inhibitors of the PI3K/AKT/mammalian target of rapamycin (mTOR) signaling pathway. Finally, lapatinib and dacomitinib represented examples of epidermal growth factor receptor (ErbB) inhibitors. The results demonstrated that no groups of inhibitors were effective against all three cell lines. JXQ-3D-4786R was sensitive to ErbB inhibitors, and particularly insensitive to mTOR inhibitors. JXQ-3D-4494R was sensitive to most of the inhibitors, and especially sensitive to cell cycle inhibitors and ErbB inhibitors. Finally JXQ-3D-902R4 was particularly sensitive to mTOR inhibitors, whereas it was insensitive to cell cycle inhibitors and ErbB inhibitors (*Figure 4*).

Discussion

In this study, we successfully established and characterized three GBC PDCs from three patients. Human GBC is a rare and highly fatal malignancy of the biliary tract with unclear biological mechanisms and poor prognosis. Due to the diagnosis at late stages of GBC, disappointing outcomes often result from surgical resection, chemotherapy and radiotherapy (24,25). Consequently, it is important to better elucidate the mechanisms of GBC invasion and metastasis to improve the prognosis of GBC in the future.

The progress of cell-culture technology has facilitated the possibility of establishing a variety of human carcinoma cell lines from surgical and autopsy tissues, biopsy specimens and peritoneum effusion. Permanent cell lines established from human cancers play a major role in basic scientific studies. According to previous reports, there are already some established cancer PDCs (16). But compared to other

Table 4 Glycosylation of three GBC PDCs

Variable	JXQ-3D-902R4	JXQ-3D-4494R	JXQ-3D-4786R
Unique glycans	10	4	7
Sialylation ratio	63%	42%	51%
Core fucosylation ratio	56%	67%	62%

The value of the sialylation ratio is the proportion of sialylated N-glycans among all the detected glycans for each PDC. The value of core fucosylation ratio is the ratio of glycans with a fucose residue in the reducing terminal among all the detected glycans for each PDC. GBC, gallbladder carcinoma; PDCs, patient-derived primary cell lines.
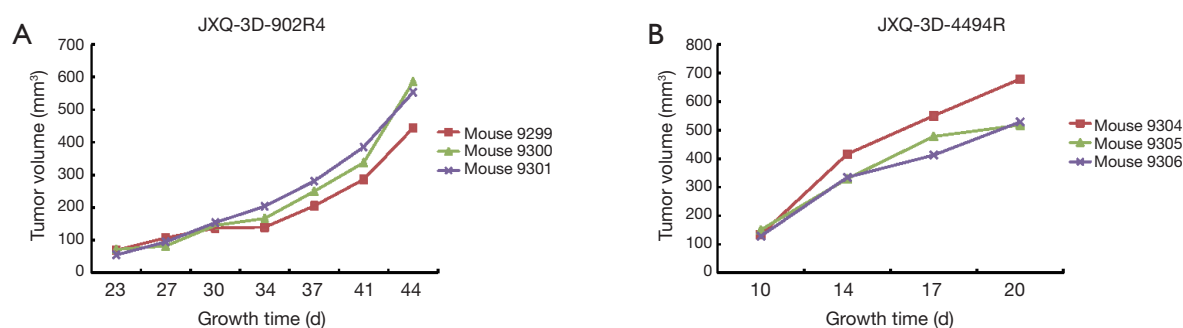
Figure 3 Tumorigenicity of three GBC PDCs in naked mice. JXQ-3D-902R4, JXQ-3D-4494R and JXQ-3D-4786R were subcutaneously transplanted into nude mice for tumorigenesis observation. Transplanted xenografts volume which grew up to over 500 mm^3 in 44 days and kinetic growth curve is shown. 9299, 9300 and 9301 are the mouse number labels (A). The transplanted xenografts of JXQ-3D-4494R grew up to a similar tumor volume in 20 days. 9304, 9305 and 9306 are also the mouse number labels (B). However, JXQ-3D-4786R did not grow to form any tumors *in vivo* due to the poor growth rate. GBC, gallbladder carcinoma; PDC, patient-derived primary cell line.

types of cancer, there are relatively few available GBC PDCs (26). Gallbladder adenocarcinomas are the major type of GBC, comprising approximately 80–97% of GBCs (27). We successfully established three PDCs, which were all derived from patients with gallbladder adenocarcinomas. Our present study comprehensively described the characteristics of the three PDCs *in vitro*, including the glycosylation modifications of total proteins. The three primary PDCs showed morphological heterogeneity with different cell shapes (*Figure 1A*). The growth rates were also different. JXQ-3D-4786R grew at the lowest speed, whereas JXQ-3D-4494R grew at the highest speed (*Figure 1B,C*). We also detected the growth activity of the three cell lines *in vivo*. Our tumorigenesis assay *in vivo* showed the same trend that we found *in vitro*. That is, JXQ-3D-4494R and JXQ-3D-902R4 grew quickly to successfully form tumors subcutaneously in naked mice, whereas— due to it having the slowest growth rate—JXQ-3D-4786R did not form any tumors subcutaneously in naked mice (*Figure 2*). These results demonstrate the heterogeneity of growth ability within the three PDCs. In this study, we first

described the characteristics of glycosylation modification of the PDCs. From these results, we found the unique glycans, sialylation ratio and core fucosylation ratio of each PDC (*Table 4*). The glycosylation-modification features reveal the uniqueness of each PDC, and the glycosylation of the whole proteins also provide novel clues for future functional studies. Glycosylation reflects the coordinated effort of a complex array of enzymes, organelles, and other factors that are needed to successfully generate carbohydrate-associated post-translational modifications. Due to the significant role of glycans in the molecular composition of a glycoprotein, alterations in glycosylation can significantly impact overall glycoprotein charge and conformation and therefore readily alter its biological activity. Furthermore, branches are biosynthesized with the help of a particular glycosyltransferase, and relatively simple changes in one glycosyltransferase can impact the biology of many different proteins in meaningful ways, thus enabling rather subtle genetic changes to induce highly pleiotropic effects on cancer cell survival and overall progression (28,29). In this study, we explored the glycosylation characteristics
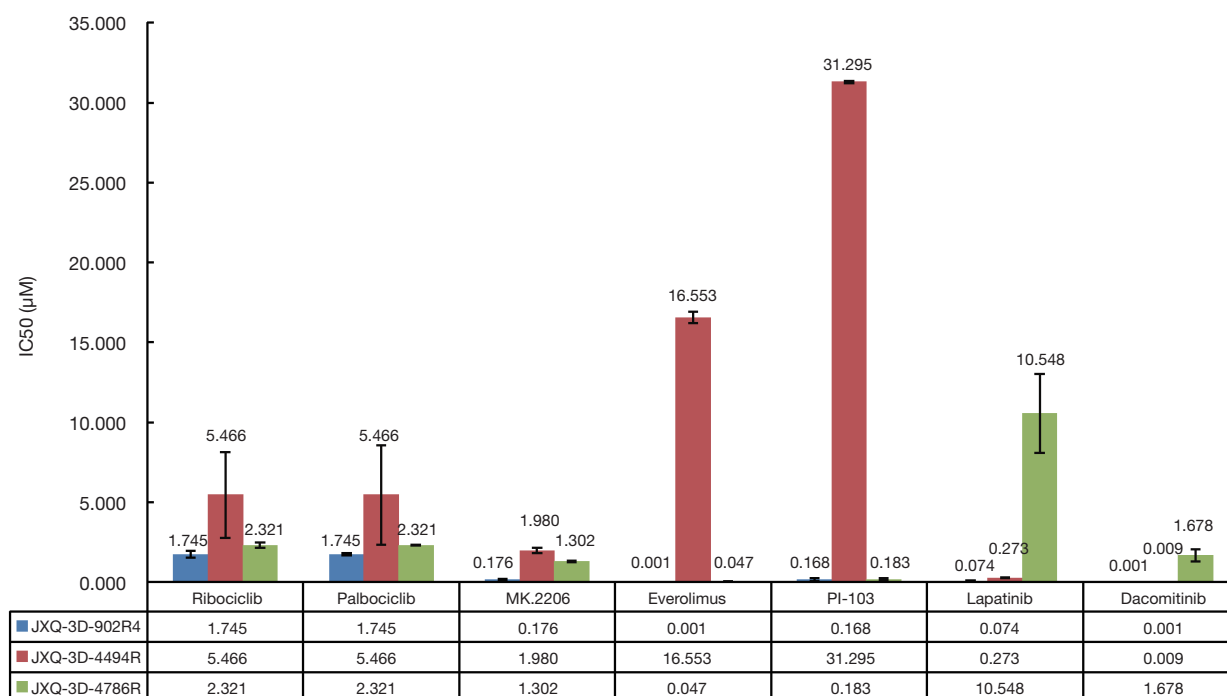
Figure 4 Sensitivities of the three PDCs to targeted drugs for gallbladder carcinoma. Fifty percent growth inhibitory concentrations (IC50s) of seven-drugs—ribociclib, palbociclib, MK2206, everolimus, PI-103, lapatinib and dacomitinib—on JXQ-3D-902R4, JXQ-3D-4494R and JXQ-3D-4786R are indicated. Ribociclib and palbociclib were cell cycle inhibitors; MK2206, everolimus and PI-103 were inhibitors of the PI3K/AKT/mTOR signaling pathway; lapatinib and dacomitinib were ErbB inhibitors. This experiment was biologically replicated three times. The original cell density of the three PDCs: JXQ-3D-4494R, 1,000 cells/well; JXQ-3D-4786R, 4,000 cells/well; JXQ-3D-902R4, 2,000 cells/well. Cell viability was measured after 144 h incubation. Error bars represent mean +/– SD from three replicates. The numbers in the table are the IC50s (µM) of the seven drugs. GBC, gallbladder carcinoma; PDC, patient-derived primary cell line; IC50, Fifty percent growth inhibitory concentrations; ErbB, epidermal growth factor receptor; mTOR, mammalian target of rapamycin.

of the three PDCs. The limitations of the assay were that we described only the glycan features. Due to the absence of normal gallbladder cells as controls, it was difficult to further investigate the biological and clinical significance of the glycosylation.

Development of medicines for cancer therapy has been hampered by a lack of preclinical models. An appropriate preclinical tool could reliably predict the efficacy of novel drugs in cancer therapy. Patient-derived tumor xenografts (PDXs) or cells (PDCs) are regarded as appropriate tools and models for basic clinical research and have been increasingly employed over the last few decades (30-33). In the present study, we presented the efficacy outcome of seven chemo-drugs evaluated by our three successfully established PDCs. The seven compounds belong to the following three groups: cell cycle inhibitors, PI3K/AKT/mTOR signaling-pathway inhibitors, and ErbB inhibitors.

The *in vitro* anti-proliferation assay in all of the PDCs indicated the different sensitivities of the three PDCs to the seven-most used chemo-drugs. None of the drugs were effective against all three PDCs (*Figure 4*). After comprehensive evaluation and comparison of the IC50 values of the seven drugs against the three PDCs, we recommend that MK2206 and Dacomitinib should be used for further research because both drugs exhibited the highest relative inhibitory effect against all of the three PDCs. Considering the complexity of the development of chemoresistance, PDCs may be qualified as preclinical research models to assess the efficacy of cancer medicines.

In conclusion, we successfully established and characterized three PDCs derived from GBC patients. The three PDCs presented herein enrich the pool of primary cell lines of GBC. In this study, we described their morphology and growth characteristics, and we first demonstrated their

glycosylation-modification features. Finally, we used these well-characterized PDCs to evaluate the efficacy of seven targeted drugs. These results suggest that these PDCs have the potential to be valuable tools for preclinical studies of targeted therapies for human GBC.

Acknowledgments

Footnote

Conflicts of Interest: All authors have completed the ICMJE uniform disclosure form (available at http://dx.doi.org/10.21037/tcr.2020.02.04). The authors have no conflicts of interest to declare.

Ethical Statement: The authors are accountable for all aspects of the work in ensuring that questions related to the accuracy or integrity of any part of the work are appropriately investigated and resolved. The study was conducted in accordance with the Declaration of Helsinki (as revised in 2013). Gallbladder carcinoma tissues of patients were collected with ethics approval obtained from the Eastern Hepatobiliary Surgery Hospital (No. EHBHKY2015-02-010), and informed consent was obtained from the patients for PDC culture and further research.

References

1. Hundal R, Shaffer EA. Gallbladder cancer: epidemiology and outcome. Clin Epidemiol 2014;6:99-109.
2. Lazcano-Ponce EC, Miquel JF, Munoz N, et al. Epidemiology and molecular pathology of gallbladder cancer. CA Cancer J Clin 2001;51:349-64.
3. Shen HX, Song HW, Xu XJ, et al. Clinical epidemiological survey of gallbladder carcinoma in northwestern China, 2009-2013: 2379 cases in 17 centers. Chronic Dis Transl Med 2017;3:60-6.
4. de Groen PC, Gores GJ, LaRusso NF, et al. Biliary tract cancers. N Engl J Med 1999;341:1368-78.
5. Hueman MT, Vollmer CM Jr, Pawlik TM. Evolving treatment strategies for gallbladder cancer. Ann Surg Oncol 2009;16:2101-15.
6. Miyakawa S, Ishihara S, Horiguchi A, et al. Biliary tract cancer treatment: 5,584 results from the Biliary Tract Cancer Statistics Registry from 1998 to 2004 in Japan. J Hepatobiliary Pancreat Surg 2009;16:1-7.
7. Hong EK, Kim KK, Lee JN, et al. Surgical outcome and prognostic factors in patients with gallbladder carcinoma. Korean J Hepatobiliary Pancreat Surg 2014;18:129-37.
8. Zhu AX, Hong TS, Hezel AF, et al. Current management of gallbladder carcinoma. Oncologist 2010;15:168-81.
9. Sekine S, Shimada Y, Nagata T, et al. Establishment and characterization of a new human gallbladder carcinoma cell line. Anticancer Res 2012;32:3211-8.
10. Kodack DP, Farago AF, Dastur A, et al. Primary Patient-Derived Cancer Cells and Their Potential for Personalized Cancer Patient Care. Cell Rep 2017;21:3298-309.
11. Pan C, Kumar C, Bohl S, et al. Comparative proteomic phenotyping of cell lines and primary cells to assess preservation of cell type-specific functions. Mol Cell Proteomics 2009;8:443-50.
12. Alge CS, Hauck SM, Priglinger SG, et al. Differential protein profiling of primary versus immortalized human RPE cells identifies expression patterns associated with cytoskeletal remodeling and cell survival. J Proteome Res 2006;5:862-78.
13. Bissig-Choisat B, Kettlun-Leyton C, Legras XD, et al. Novel patient-derived xenograft and cell line models for therapeutic testing of pediatric liver cancer. J Hepatol 2016;65:325-33.
14. Chapuy B, Cheng H, Watahiki A, et al. Diffuse large B-cell lymphoma patient-derived xenograft models capture the molecular and biological heterogeneity of the disease. Blood 2016;127:2203-13.
15. Nicolle D, Fabre M, Simon-Coma M, et al. Patient-derived mouse xenografts from pediatric liver cancer predict tumor recurrence and advise clinical management. Hepatology 2016;64:1121-35.
16. Liu ZY, Xu GL, Tao HH, et al. Establishment and characterization of a novel highly aggressive gallbladder cancer cell line, TJ-GBC2. Cancer Cell Int 2017;17:20.

17. Li QK, Chen L, Ao MH, et al. Serum fucosylated prostate-specific antigen (PSA) improves the differentiation of aggressive from non-aggressive prostate cancers. Theranostics 2015;5:267-76.

18. Zhao Q, Zhan T, Deng Z, et al. Glycan analysis of colorectal cancer samples reveals stage-dependent changes in CEA glycosylation patterns. Clin Proteomics 2018;15:9.

19. Yang G, Tan Z, Lu W, et al. Quantitative glycome analysis of N-glycan patterns in bladder cancer vs normal bladder cells using an integrated strategy. J Proteome Res 2015;14:639-53.

20. Sethi MK, Thaysen-Andersen M, Smith JT, et al. Comparative N-glycan profiling of colorectal cancer cell lines reveals unique bisecting GlcNAc and alpha-2,3-linked sialic acid determinants are associated with membrane proteins of the more metastatic/aggressive cell lines. J Proteome Res 2014;13:277-88.

21. Feng F, Cheng Q, Yang L, et al. Guidance to rational use of pharmaceuticals in gallbladder sarcomatoid carcinoma using patient-derived cancer cells and whole exome sequencing. Oncotarget 2017;8:5349-60.

22. Kohli M, Ho Y, Hillman DW, et al. Androgen Receptor Variant AR-V9 Is Coexpressed with AR-V7 in Prostate Cancer Metastases and Predicts Abiraterone Resistance. Clin Cancer Res 2017;23:4704-15.

23. Huang C, Liu Y, Wu H, et al. Characterization of IgG glycosylation in rheumatoid arthritis patients by MALDI-TOF-MS(n) and capillary electrophoresis. Anal Bioanal Chem 2017;409:3731-9.

24. Mastoraki A, Papanikolaou IS, Konstandiadou I, et al. Facing the challenge of treating gallbladder carcinoma. Review of the literature. Hepatogastroenterology 2010;57:215-9.

25. Shukla PJ, Barreto SG. Gallbladder cancer: we need to do better! Ann Surg Oncol 2009;16:2084-5.

26. Khan SA, Thomas HC, Davidson BR, et al. Cholangiocarcinoma. Lancet 2005;366:1303-14.

27. Goetze TO. Gallbladder carcinoma: Prognostic factors and therapeutic options. World J Gastroenterol 2015;21:12211-7.

28. Fuster MM, Esko JD. The sweet and sour of cancer: glycans as novel therapeutic targets. Nat Rev Cancer 2005;5:526-42.

29. Cummings RD, Pierce JM. The challenge and promise of glycomics. Chem Biol 2014;21:1-15.

30. Pandrangi SL, Raju Bagadi SA, Sinha NK, et al. Establishment and characterization of two primary breast cancer cell lines from young Indian breast cancer patients: mutation analysis. Cancer Cell Int 2014;14:14.

31. Tentler JJ, Tan AC, Weekes CD, et al. Patient-derived tumour xenografts as models for oncology drug development. Nat Rev Clin Oncol 2012;9:338-50.

32. Siolas D, Hannon GJ. Patient-derived tumor xenografts: transforming clinical samples into mouse models. Cancer Res 2013;73:5315-9.

33. Julien S, Merino-Trigo A, Lacroix L, et al. Characterization of a large panel of patient-derived tumor xenografts representing the clinical heterogeneity of human colorectal cancer. Clin Cancer Res 2012;18:5314-28.

	1	2	3	4	5	6	7	8	9	10	11	12
A												
B												
C	JXQ-3D-902R4	4000	4000	4000	2000	2000	2000	1000	1000	1000	NcC	
D	JXQ-3D-4494R	4000	4000	4000	2000	2000	2000	1000	1000	1000	NcC	
E	JXQ-3D-4786R	4000	4000	4000	2000	2000	2000	1000	1000	1000	NcC	
F												
G												
H												

Figure S1 The experimental design of cell proliferation assay. The numbers in the image represent the cell density used in the experiment, unit: cells/well. NcC, no cell control.
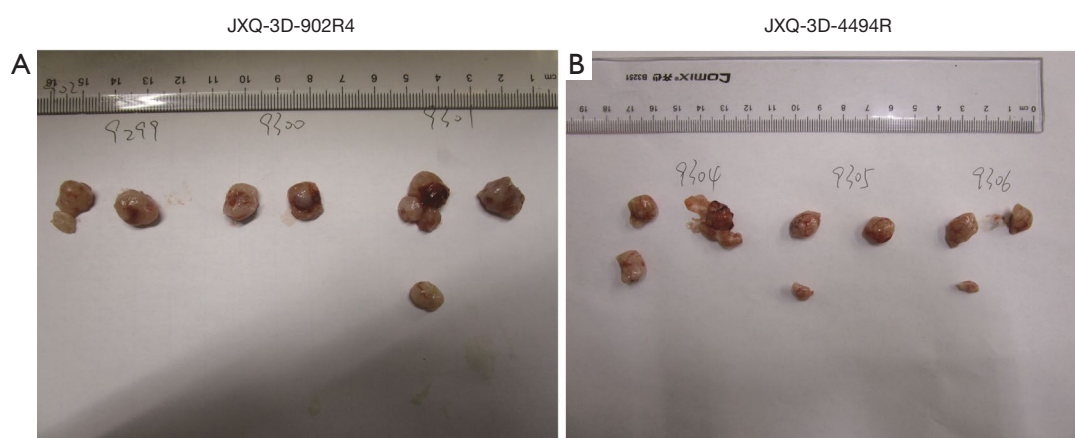
Figure S2 Images of transplanted xenografts of JXQ-3D-902R4 (A) and JXQ-3D-4494R (B).

Table S1 STR loci analysis for primary tissues of three established GBC PDCs

STR locus	JXQ-3D-902R4	JXQ-3D-4494R	JXQ-3D-4786R
Amelogenin	X	X, Y	X, Y
D5S818	11, 12	11, 12	11, 13
D13S317	9, 11	8, 12	8, 10
D7S820	8, 12	8, 11	8, 11
D16S539	10, 11	9, 12	10, 13
vWA	16, 19	16	17, 18
TH01	9	7	7
TPOX	8, 12	9, 12	8
CSF1PO	12	9, 12	11
D12S391	20, 22	18, 19	19, 20
FGA	22, 25	23, 27	22
D2S1338	19, 23	19, 23	19, 24
D21S11	31, 32	31, 33.2	29, 32.2
D18S51	17, 19	17	14, 23
D8S1179	13, 14	12, 15	14
D3S1358	15	14, 18	16, 17
D6S1043	11	18	10, 14
PENTAE	12, 13	12, 21	12, 17
D19S433	15.2	12, 14	13, 15.2
PENTAD	8, 13	9	11, 12

GBC, gallbladder carcinoma; PDC, patient-derived primary cell line; STR, short tandem repeat.

Table S2 The expression levels of coding genes of typical epithelial markers cytokeratin-7, 8, 18 and 19, negative control CD34, and mesenchymal marker vimentin in the three PDCs were studied using RNA-seq. Each PDC was assessed three times in parallel

Gene	JXQ-3D-4494R-1	JXQ-3D-4494R-2	JXQ-3D-4494R-3	JXQ-3D-4786R-1	JXQ-3D-4786R-2	JXQ-3D-4786R-3	JXQ-3D-902R4-1	JXQ-3D-902R4-2	JXQ-3D-902R4-3
KRT7	700.28	669.813	720.693	1,107.91	1,125.34	1,134.48	1,179.14	1,109.07	1,243.15
KRT8	380.893	383.784	395.832	338.43	336.079	344.675	812.417	760.385	842.105
KRT18	307.122	297.565	304.337	141.444	146.995	146.672	949.329	910.485	962.935
KRT19	801.223	798.285	837.328	2,477.54	2,406.53	2,478.08	481.031	443.964	493.705
CD34	0.150532	0.124826	0.167466	0	0.0405161	0.0428595	0.0168717	0.0168319	0.0383703
VIM	3.9862	3.98274	4.03764	0.144452	0.152615	0.125598	14.813	15.12	13.5235

KRT7, *KRT8*, *KRT18* and *KRT19* are coding genes of epithelial markers of cytokeratin-7, 8, 18 and 19; *VIM* is coding gene of mesenchymal marker vimentin. *CD34* is the negative control. PDC, derived primary cell.